Calculating the Susceptibility of Carbon Steels to Solidification Cracking During Welding



CHUNZHI XIA and SINDO KOU

Existing experimental results of weldability tests show the susceptibility of carbon steels to solidification cracking varies significantly with the C content. To analyze the effect of the C content on the susceptibility, equilibrium solidification of binary Fe-C alloys was assumed as an approximation in view of the rapid diffusion of the interstitial solute C in Fe. First, the curve of the equilibrium freezing temperature range vs. the C content was plotted and compared with the experimental results, but the agreement was not good. Then, the susceptibility index, i.e., $|dT/d(f_S)^{1/2}|$ near $(f_S)^{1/2} = 1$ (T: temperature; f_S : fraction solid) recently proposed for Al alloys was tried. The curve of the susceptibility index vs. the C content was calculated. The curve agreed well with the experimental results of crack susceptibility tests of carbon steels in welding.

https://doi.org/10.1007/s11663-020-02021-5
© The Minerals, Metals & Materials Society and ASM International 2021

I. INTRODUCTION

CRACKING can occur in the mushy zone during solidification, called solidification cracking in welding and hot tearing in casting. It occurs along boundaries of columnar dendritic grains under the tension induced by solidification shrinkage and thermal contraction.^[1] Various weldability tests have been used to evaluate the susceptibility of alloys to solidification cracking. The most widely used test is the Varestraint test. [2] A horizontal plate is bent downward suddenly during welding against a curved block to induce tension in the plate and hence the mushy zone to cause cracking. The greater the maximum or total crack length is under a given tension (i.e., for a given plate thickness and radius of the bending block), the higher the crack susceptibility. Although the tension at the top surface of the plate is known, the tension in the mushy zone that causes cracking is unknown. The transverse-motion weldability (TMW) test is a newest test developed recently by Soysal and Kou. [3,4] This is a simple lap welding experiment illustrated in Figure 1. The upper sheet is stationary while the lower sheet is moved at a constant speed V in the transverse direction of welding to induce tension in the mushy zone alone to cause cracking. The slower the lower-sheet V is required to cause cracking, the higher the crack susceptibility. The nominal horizontal tensile

Kou^[10] recently proposed a criterion for solidification cracking. Based on the criterion, an index was further proposed for predicting the susceptibility to solidification cracking. [10,11] The validity of the index was verified against welds of Al alloys, [4,12-16] Mg alloys, [6] Ni-base alloys, [8] and Al filler-metal guides. [17,18] The criterion for cracking is illustrated in Figure 2(a), where a volume element Ω is shown between the roots of two columnar dendritic grains near the centerline of the mushy zone. For mathematical analysis, the grains near the centerline can be imagined to be growing inside an array of hexagonal tubes along the welding direction. [10]

Three factors can affect if a void (crack) can form in the volume element. Factor 1 is the volumetric rate of space increase in Ω caused by the transverse tensile strain. Factor 2 is the volumetric rate of space decrease in Ω caused by the lateral growth of the grains. Factor 3 is the volumetric rate of space decrease in Ω caused by liquid entering Ω minus liquid leaving Ω . The criterion for cracking to occur is that Factor 1 exceeds the sum of Factors 2 and 3. Although liquid has no strength to resist cracking, it can feed the space in Ω to keep a void,

strain rate at the top surface of the mushy zone is the horizontal width of the weld divided by V. Unlike the Varestraint test,^[2] the TMW test can induce solidification cracking by applying tension slowly and a filler metal can be used during welding to evaluate its effect on solidification cracking. The TMW test requires no pneumatic system and bending blocks, only a motor. It also requires much less workpiece material. The TMW test has been applied to Al alloys,^[3–5] Mg alloys,^[6] stainless steels,^[7] Ni-base alloys^[8] and carbon steels.^[9] The validity of the TMW test^[3–9] has been verified by the results of other weldability tests and by filler metal guides.

CHUNZHI XIA is with the Department of Materials Science and Engineering, Jiangsu University of Science and Technology, Zhenjiang 212003, China. SINDO KOU is with the Department of Materials Science and Engineering, The University of Wisconsin, Madison, WI 53706, USA. Contact e-mail: kou@engr.wisc.edu

Manuscript submitted August 17, 2020, Accepted October 25, 2020. Article published online January 2, 2021.

i.e., crack, from being created. An equation was derived for the criterion based on the conservation of space. [10] Cracking can occur if crack initiation sites are available, such as micro porosity or folded oxide films[19,20] or external surfaces.[21]

Kou^[10] proposed $|dT/d(f_S)^{1/2}|$ near $(f_S)^{1/2} = 1$ as the index for the susceptibility of Al alloys to solidification cracking, where T is temperature and f_S the fraction of solid. The higher the index is, the greater the crack

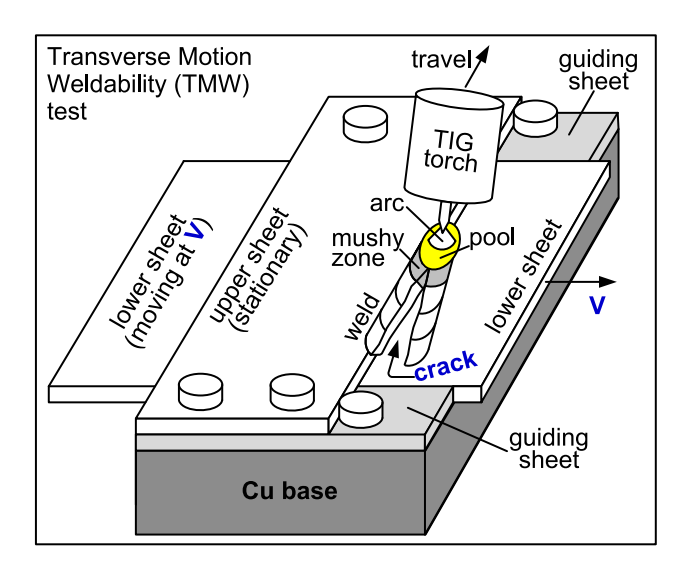


Fig. 1—Transverse motion weldability test.^[3,4] The lower sheet is moved in the transverse direction of welding to induce solidification cracking.

susceptibility becomes. The index is explained in Figure 2(b). Let R be the characteristic radius of columnar grains near $f_{\rm S}=1$. As an approximation, he showed R is proportional to $(f_{\rm S})^{1/2}$. Thus, for a given temperature drop $|{\rm d}T|$ during cooling, a high $|{\rm d}T/{\rm d}(f_{\rm S})^{1/2}|$ suggests a very small lateral growth dR. So, lateral growth is very slow, and Factor 2 is small. Since the grains grow thicker very slowly as they grow longer, the liquid channels between the grains becomes very long, which slows down the liquid feeding needed to resist cracking. [22] So, Factor 3 is also small. Thus, the higher $|{\rm d}T/{\rm d}(f_{\rm S})^{1/2}|$ is near $(f_{\rm S})^{1/2}=1$, the more likely Factor 1 can exceed Factor 2 plus Factor 3.

Since the maximum steepness $|dT/d(f_S)^{1/2}|$ occurs near $(f_S)^{1/2}=1$, the maximum steepness can also be used as the index. Based on the observation of Fisher and Kurz, are extensive bonding between columnar dendrites can occur at $f_S=0.98$, that is, $(f_S)^{1/2}=0.99$. Thus, Kou also proposed to use the maximum $|dT/d(f_S)^{1/2}|$ up to $(f_S)^{1/2}=0.99$ as a simple index for the crack susceptibility of Al alloys. Beyond $(f_S)^{1/2}=0.99$, solidification cracking is unlikely because of extensive bonding between grains. As mentioned previously, the validity of the index has been verified against Al welds. As more expression of the index has been used by other investigators. The crack susceptibility index proposed by Kou has also been used by other investigators.

In the present study, the maximum $|dT/d(f_S)^{1/2}|$ near $(f_S)^{1/2} = 1$ was applied to carbon steels as the susceptibility index and was calculated based on equilibrium solidification, *i.e.*, complete diffusion of C in both liquid and solid iron.

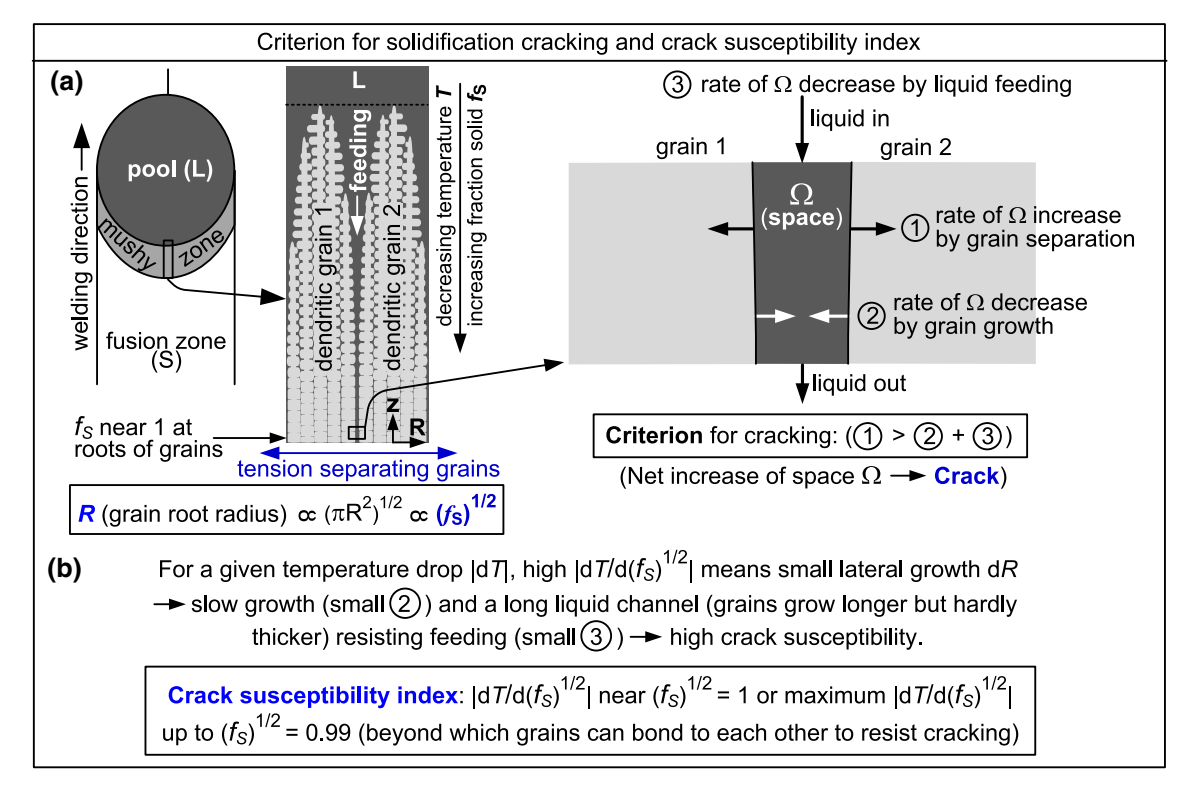


Fig. 2—Solidification cracking model proposed by Kou^[10]: (a) criterion for cracking and (b) index for crack susceptibility.

II. PROCEDURE

The thermodynamics software Pandat^[28] and the Fe database PanIron^[29] of CompuTherm, LLC, Madison, WI were used to calculate the binary Fe-C phase diagram. The equilibrium solidification model was then used, that is, assuming complete diffusion in both liquid and solid, to calculate the fraction of solid f_S as a function of temperature T for binary Fe-C alloys of various C contents. The curves of T vs. f_S , i.e., the solidification paths, of the Fe-C alloys were plotted. The curves of T vs. $(f_S)^{1/2}$ were also plotted. Extensive bonding between grains was assumed to occur at $f_S = 0.98$, i.e., $(f_S)^{1/2} = 0.99$. Thus, the maximum steepness $|dT/d(f_S)^{1/2}|$ up to $(f_S)^{1/2} = 0.99$ was taken as the crack susceptibility index. The index was then plotted as a function of the C content, that is, the crack susceptibility curve of Fe-C alloys.

III. RESULTS AND DISCUSSION

A. Equilibrium Freezing Temperature Range

The calculated binary Fe-C phase diagram is shown in Figure 3(a). It shows three phases in equilibrium with each other at the peritectic temperature 1494.6 °C. They are δ -ferrite at its maximum C solubility 0.093 wt pct C, austenite γ at the peritectic point 0.172 wt pct C, and the liquid phase L at 0.528 wt pct C. The assumption of complete diffusion in both liquid and solid, i.e., equilibrium solidification, is based on the fact that C is an interstitial solute in Fe. At a given C content, the equilibrium freezing temperature range is from the liquidus temperature to the solidus temperature at the C content. As shown in Figure 3(b), it increases with increasing C content from zero in pure Fe to the maximum solubility of δ -ferrite at 0.093 wt pct C, decreases with increasing C content to the peritectic point at 0.172 wt pct C, and then increases again with further increase in the C content.

Figure 4 shows the experimental results of the Varestraint test and the TMW test of carbon steels. The closed circles indicate the TMW test results of Xia and Kou, [9] shown by plotting the lower-sheet speed V vs. the C content. As mentioned previously, the slower the lower-sheet V is required to cause cracking, the higher the crack susceptibility. In Figure 4 V is plotted to increase from top to bottom, so that crack susceptibility is higher near the top and lower near the bottom, consistent with results of other tests shown in the same figure. In the TMW test of a given material, a crack initiated does not propagate at all when V is low and propagates all the way to the end of the weld (i.e., full propagation) when V is high. Thus, there exists a range of V where crack propagation changes from none to full crack propagation, i.e., the transition range. In Figure 4 the transition range of each carbon steel tested is indicated by a vertical bar, with a closed circle shown at the midpoint of the range. Thus, a bar located closer to the top of the figure indicates a higher crack susceptibility.

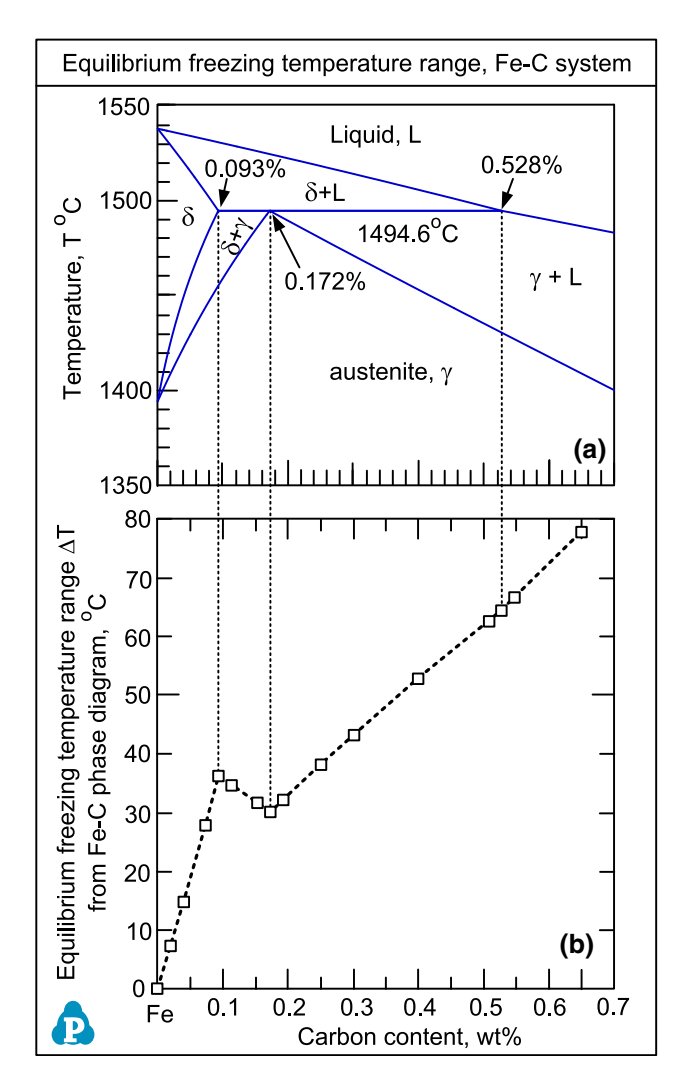


Fig. 3—Binary Fe-C system: (a) phase diagram and (b) equilibrium freezing temperature range ΔT (from liquidus to solidus). Calculated using Pandat^[28] and PanIron^[29]

In Figure 4 the open circles indicate the results of Shankar and Devletian^[30] based on the longitudinal version of the Varestraint test. [2] The open triangles are also the results of Shankar and Devletian^[30] but based on the transverse version of the Varestraint test.^[31] Both sets of results are shown by plotting the maximum crack length vs. the C content. The closed triangles indicate the results of Matsuda et al. [32] based on in situ observation and measurement during the tensile hot cracking test of plain carbon steels, shown by plotting the minimum strain required to cause cracking vs. the C content. Welding was conducted along the centerline of a horizontal tensile-test specimen pulled in the transverse direction of welding. The lower the minimum strain was needed to cause cracking, the higher the crack susceptibility. As can be seen, the experimental results of the weldability tests shown in Figure 4 are essentially consistent with each other except for the three points of Shankar and Devletian^[30] encircled by the oval, which seem consistent neither with the results of Matsuda et al. [32] nor those of the TMW test. [9]

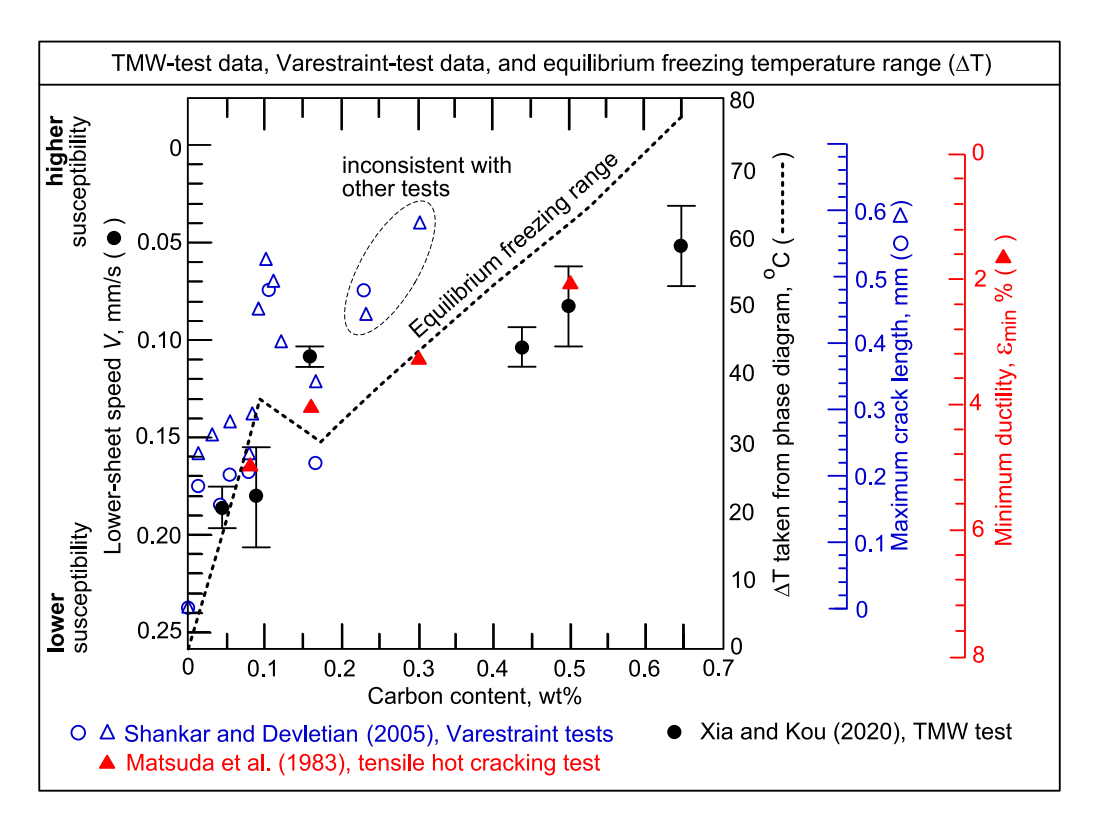


Fig. 4—Comparing susceptibility to solidification cracking based on TMW test, Varestraint tests, tensile hot cracking test, and equilibrium freezing temperature range ΔT .

Table I. Chemical Compositions (Wt Pct) of the Carbon Steels Tested by Xia and Kou^[9]

Carbon Steels	C	Mn	Si	P	S	Fe
04C 09C 16C 44C 50C 65C	0.044 0.09 0.16 0.44 0.50 0.65	0.20 0.29 0.77 0.89 0.69 1.04	0.02 0.02 0.01 0.21 0.24 0.23	0.004 0.023 0.010 0.014 0.010 0.015	0.002 0.009 0.007 0.0001 0.003 0.001	balance balance balance balance balance

The thick dotted line in Figure 4 is the curve of the equilibrium freezing temperature range ΔT vs. the C content. As an approximation, the carbon steels in the present study are taken as binary Fe-C alloys, neglecting their very low S and P, and relatively low Si and Mn (Table I). However, the equilibrium freezing temperature range does not correlate with the experimental results.

B. Index for Solidification-Cracking Susceptibility

The index for the susceptibility to solidification cracking recently proposed by Kou,^[11] *i.e.*, the maximum values of $|dT/d(f_S)^{1/2}|$ up to $(f_S)^{1/2}=0.99$, is explored as follows. Figure 5 shows example $T-f_S$ curves of several binary Fe-C alloys. The arrowheads along the curves indicate the points where new solid phases start to form from the liquid phase (L) during solidification.

Figure 6 shows the curves of T vs. $(f_{\rm S})^{1/2}$ beyond $(f_{\rm S})^{1/2}$ = 0.90 based on the T– $f_{\rm S}$ curves in Figure 5. The short straight lines are the tangents showing the maximum steepness $|{\rm d}T/{\rm d}(f_{\rm S})^{1/2}|$ up to $(f_{\rm S})^{1/2}=0.99$, that is, the index for the susceptibility to solidification cracking. The index is plotted vs. the C content in Figure 6(h). The "N-shaped" curve shows a peak at 0.093 wt pct C (the maximum C solubility in δ -ferrite) and a minimum at 0.192 wt pct C (slightly beyond the peritectic composition 0.172 wt pct C).

In Figure 7 the curve of the calculated susceptibility index vs. the C content (dotted thick line) is compared with the results of the TMW test and the Varestraint tests. As shown, the curve correlates well with the results of the TMW test and the Varestraint tests, except for the three points of Shankar and Devletian^[30] inside the oval. As can be seen, the peak of the calculated susceptibility curve at 0.093 wt pct C is very close to the peak shown by Shankar and Devletian^[30]. In the butt-welding test of low C steels, Ohshita *et al.*^[33] observed a critical C content, slightly below which solidification cracking occurred and slightly above which solidification cracking disappeared. The critical content existed between 0.08 and 0.11 wt pct C, close to the peak shown in Figure 7. As shown in Figure 6, the steepness of the $T-(f_S)^{1/2}$ curve decreases with increasing C content from 0.093 wt pct C (Figure 6(b)) through 0.192 wt pct C (Figure 6(e)). This suggests, with increasing C content from 0.093 to 0.192 wt pct C, columnar dendritic grains grow thicker faster to bond together and liquid feeds

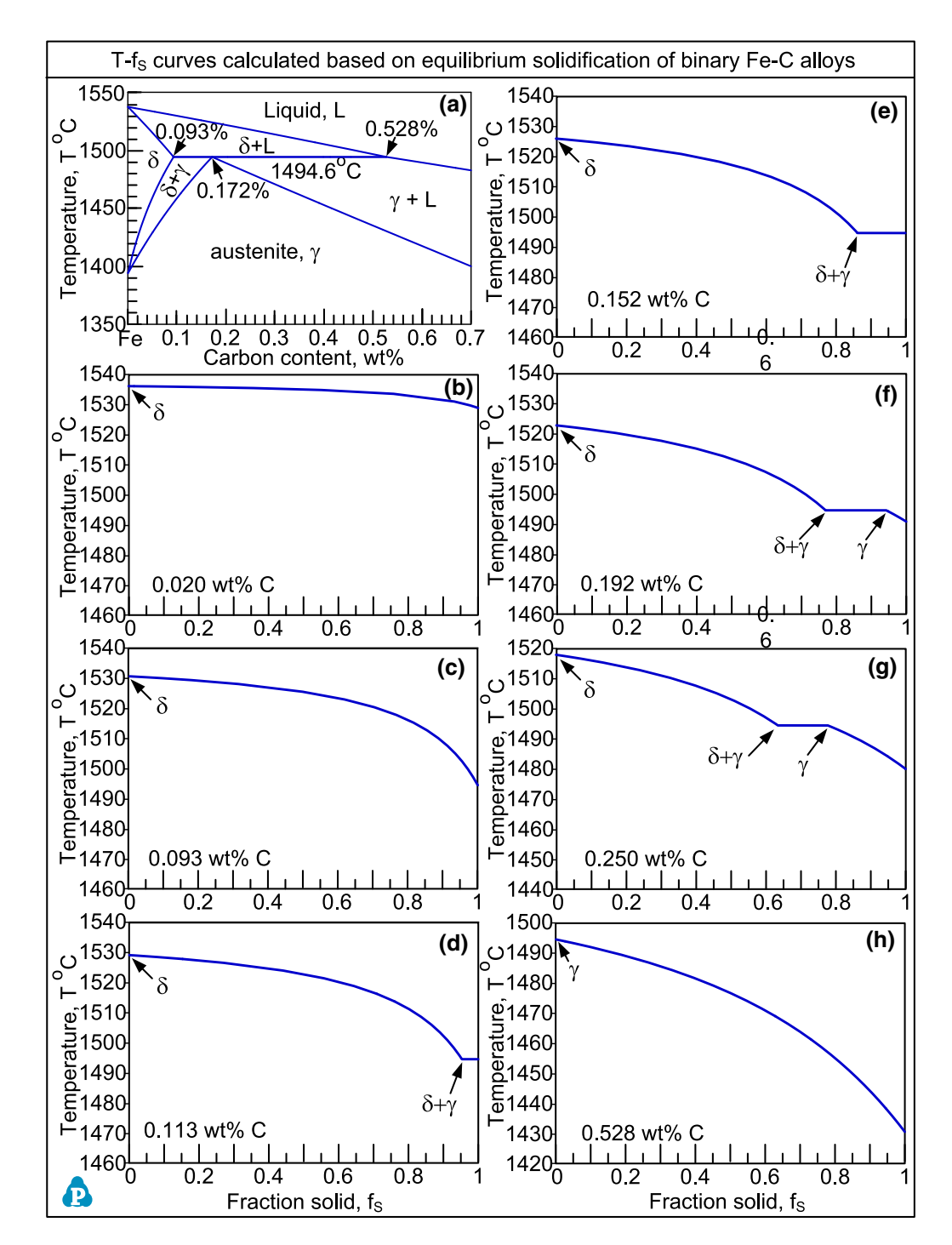


Fig. 5—Calculated paths of equilibrium solidification (*i.e.*, complete C diffusion in solids and liquid) of Fe-C alloys: (a) Fe-C phase diagram and (b) through (h) curves of T vs. f_S.

faster, thus increasing the resistance to solidification cracking. This explains the decreasing susceptibility with increasing C from 0.093 to 0.192 wt pct C.

As can also be seen in Figure 7, the calculated susceptibility curve shows a minimum at 0.192 wt pct C. In the intermittent butt-welding test of carbon steels in the range of 0.13 to 0.22 wt pct C, Amaya *et al.*^[34] showed the crack susceptibility was negligible but started to increase suddenly beyond 0.19 wt pct C. This

critical C content of 0.19 wt pct is consistent with the minimum susceptibility at 0.192 wt pct C shown in Figure 7.

Thus, the crack susceptibility curve based on the maximum $|dT/d(f_S)^{1/2}|$ from $(f_S)^{1/2} = 0.90$ to 0.99 as the susceptibility index is consistent with the results of the TMW test, [9] Varestraint tests, [30] tensile hot cracking test, [32] and butt-welding tests. [33,34] This seems to indicate that C plays a dominant role in the solidification cracking of carbon steels. However, other elements

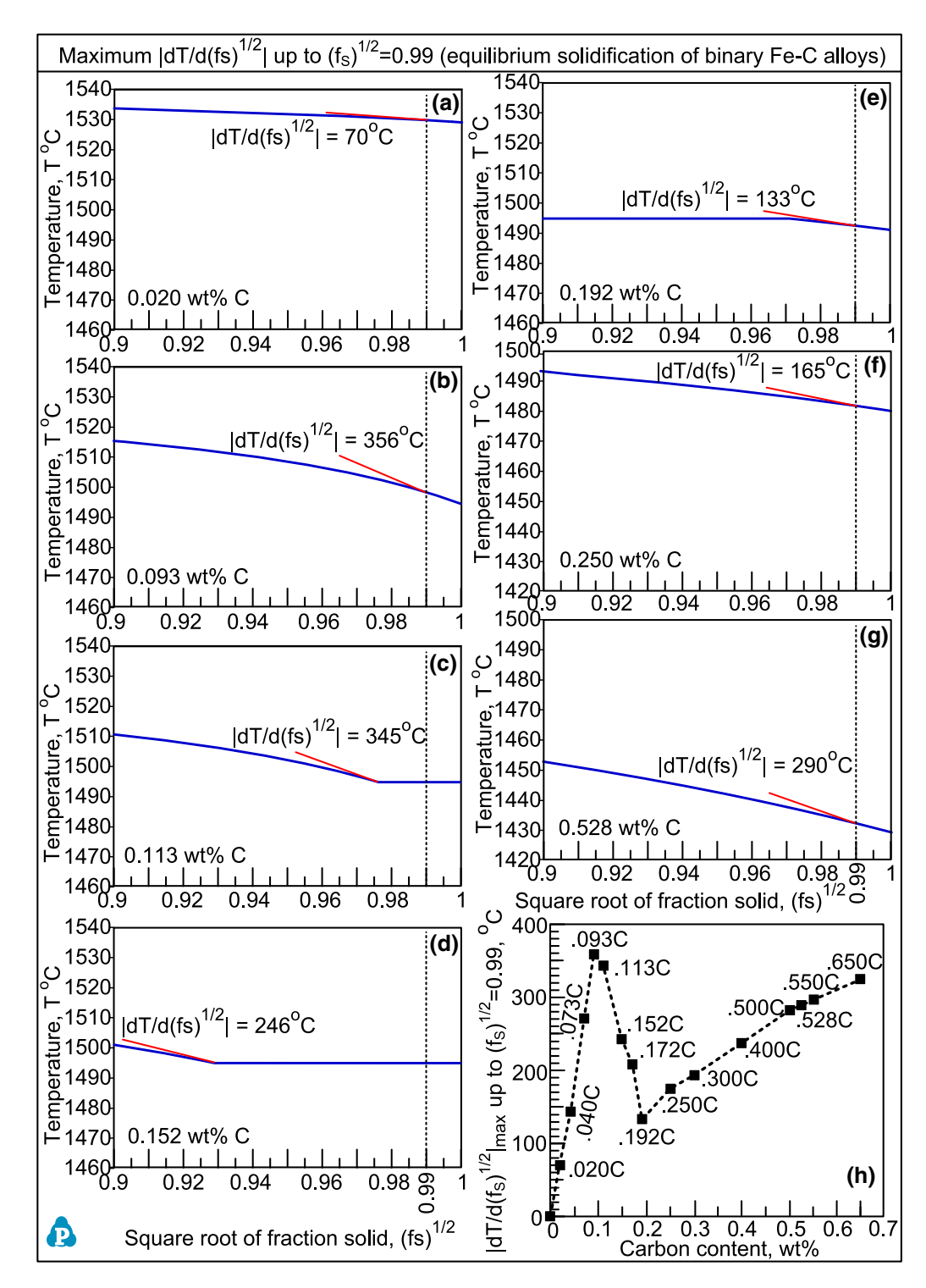


Fig. 6—Calculated crack susceptibility of Fe-C alloys: (a) through (g) maximum $|dT/d(f_S)^{1/2}|$ (from Fig. 5) up to $(f_S)^{1/2} = 0.99$ as susceptibility index and (h) calculated crack susceptibility curve.

are also present, such as Mn, Si, P and S as shown in Table I for the carbon steels used in the TMW test. [9] S and P are known to increase the crack susceptibility of steels. They affect the crack susceptibility more significantly than Mn and Si. The S content is very low (0.001 to 0.003 wt pct) except for steels 09C and 16C. Steel 09C contained 0.009 wt pct S and 0.29 wt pct Mn, and the

Mn/S ratio was 32.2. Steel 16C contained 0.007 wt pct S and 0.77 wt pct Mn, and the Mn/S ratio was 110. Smith^[35] showed no solidification cracking in carbon steels at 0.09 wt pct C if Mn/S > 9 and no cracking at 0.16 wt pct C if Mn/S > 55. Thus, S in steels 09C and 16C might not have a significant effect on their crack susceptibility. The P content was about constant at

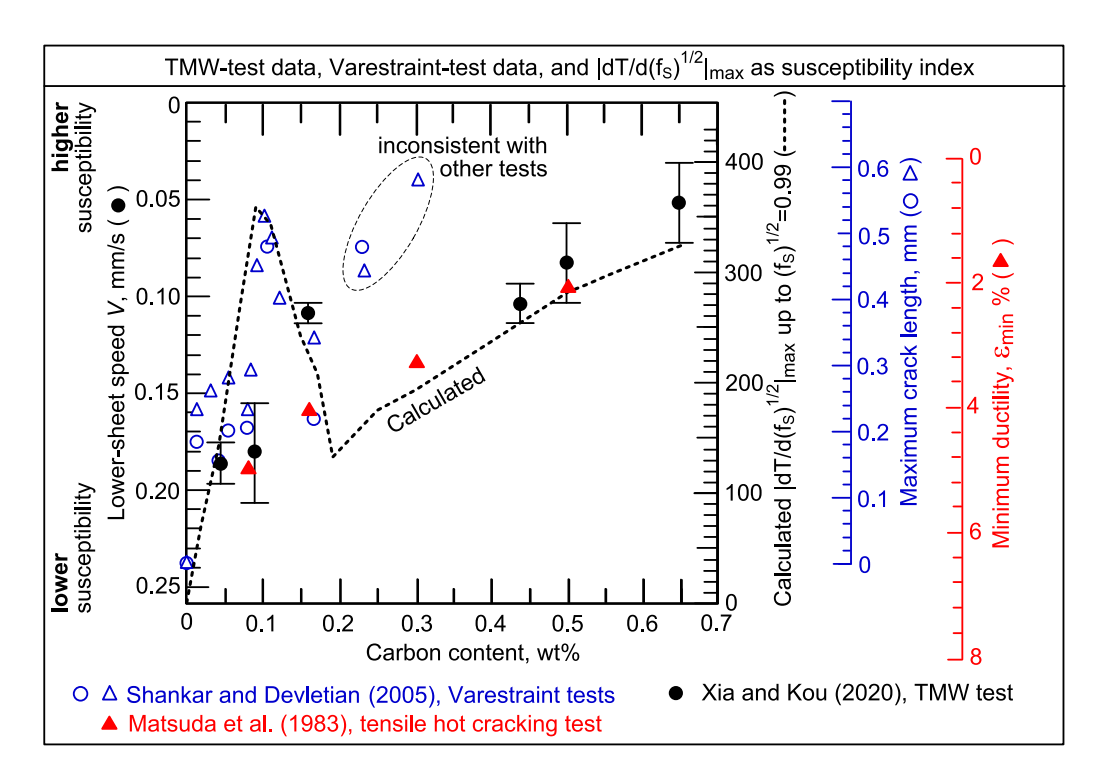


Fig. 7—Comparing results of TMW test, Varestraint tests, tensile hot cracking test, and susceptibility calculation (under equilibrium solidification).

Table II. Ferrite Potential Calculated Based Table I Using Eqs. [1] and [2]

Carbon Steels	C	+ 0.02 [Mn]	-0.1 [Si]	$C_{ m P}$	FP
04C	0.044	+ 0.004	- 0.002	0.0460	1.1350
09C	0.09	+ 0.0058	-0.002	0.0938	1.0155
16C	0.16	+ 0.0154	-0.001	0.1654	0.8365
44C	0.44	+ 0.0178	-0.021	0.4368	0.1580
50C	0.50	+ 0.0138	-0.024	0.4898	0.0255
65C	0.65	+ 0.0208	-0.023	0.6478	-0.3695

0.012 wt pct except for steel 04C (0.004 wt pct P) and steel 09C (0.023 wt pct P). Steel 09C had twice more P than steel 16C (0.010 wt pct P) but a lower crack susceptibility than steel 16C. Thus, the higher P content (0.023 wt pct) of steel 09C could not have increased its crack susceptibility significantly. The ferrite potential corresponding to Table I is shown in Table II, which will be discussed subsequently. In the Fe-C alloys of Shankar and Devletian^[30] shown in Figure 7, the S content and the P content were both below 0.001 wt pct as can be seen in Table III. The ferrite potential corresponding to Table III is shown in Table IV, which will also be discussed subsequently. In the plain carbon steels of Matsuda et al.[32], the S content was below 0.005 wt pct and the P content at 0.010 wt pct as can be seen in Table V. The ferrite potential corresponding to Table V is shown in Table VI, which will also be discussed subsequently.

Table III. Compositions (Wt Pct) of Carbon Steels Tested by Shankar and Devletian^[30]

Carbon Steels	С	Mn	Si	P	S
#9628	0.002	0	0.07	0.001	0.001
#9855	0.012	0	0.076	0	0.0005
#9937-A	0.030	0	0.07	0.001	0.0007
#9629	0.053	0	0.07	0.001	0.001
#9656	0.078	0	0.075	0	0.0008
#9637-В	0.09	0	0.07	0.001	0.0007
#9636	0.104	0	0.072	0.001	0.001
#9658	0.165	0	0.071	0	0.0004
#9631	0.228	0	0.07	0.001	0.001
#9637	0.30	0	0.07	0	0.0004

Table IV. Ferrite Potential Calculated Based Table III Using Eqs. [1] and [2]

Carbon Steels	C	+ 0.02 [Mn]	- 0.1 [Si]	$C_{ m P}$	FP
#9628	0.002	0	- 0.007	- 0.005	1.2625
#9855	0.012	0	-0.0076	0.0044	1.239
#9937-A	0.030	0	-0.007	0.023	1.1925
#9629	0.053	0	-0.007	0.046	1.135
#9656	0.078	0	-0.0075	0.0705	1.07375
#9637-В	0.09	0	-0.007	0.083	1.0425
#9636	0.104	0	-0.0072	0.0968	1.008
#9658	0.165	0	-0.0071	0.1579	0.85525
#9631	0.228	0	-0.007	0.221	0.6975
#9637	0.30	0	-0.007	0.293	0.5175

Table V. Compositions (Wt Pct) of Carbon Steels Tested by Matsuda et al. [32]

Carbon Steels	C	Mn	Si	P	S	Fe
08C	0.08	0.28	0.14	0.010	0.003	balance
16C	0.16	0.28	0.14	0.010	0.004	balance
30C	0.31	0.28	0.14	0.010	0.004	balance
50C	0.50	0.29	0.14	0.010	0.005	balance

Table VI. Ferrite Potential Calculated Based Table V Using Eqs. [1] and [2]

Carbon Steels	C	+ 0.02 [Mn]	- 0.1 [Si]	$C_{ m p}$	FP
08C	0.08	+ 0.0056	- 0.014	0.0716	1.071
16C	0.16	+ 0.0056	-0.014	0.1516	0.871
30C	0.31	+ 0.0056	-0.014	0.3016	0.496
50C	0.50	+ 0.0058	- 0.014	0.4918	0.0205

C. Further Discussion

The focus of the present study is welding instead of casting. However, it is worth mentioning that hot tearing and related issues in casting of carbon steels have been studied extensively. [36–40] Numerous examples can be found in the review by Azizi *et al.* [38] Some of the results in the present study can be related to work on steel casting as follows.

Figure 7 shows that beyond 0.2 pct C the crack susceptibility increases with increasing C content. The welding mushy zone can be expected to be longer along its centerline with a higher C content, which can be seen from the Fe-C phase diagram in Figure 3(a). In all the crack susceptibility tests involved in Figure 7, the mushy zone is subjected to applied tension, especially in the transverse direction. Thus, the mushy zone can be expected to crack to the end of its centerline. This may not be true in continuous casting where tension is not applied externally. So, beyond 0.2 pct C the crack susceptibility may increase in a weldability test but not necessarily in continuous casting.

The strain (shrinkage) induced by the $\delta \rightarrow \gamma$ transformation has been shown to play a crucial role in hot tearing in steel casting. [38] For carbon steels this shrinkage is most significant at 0.1 wt pct C.[40] Consider the 09C steel (0.09 wt pct C) in Figure 7 as an example for comparing the strain rate caused by the $\delta \rightarrow \gamma$ transformation and the strain rate in the TMW test. The equilibrium temperature range of the $(\delta + \gamma)$ region at 0.09 wt pct C, taken from the Fe-C phase diagram in Figure 5(a), is about 40 °C. Senda et al. [31] measured a cooling rate of about 267 °C/s during solidification of steel in welding. Using this cooling rate for estimation, the time to cool through the 40 °C range for the $\delta \rightarrow \gamma$ transformation in the 09C steel weld is 0.15 s (i.e., 40 °C ÷ 267 °C/s). Ohshita et al. [33] pointed out the lateral shrinkage associated with the transformation from δ -ferrite to austenite γ is 0.0011. Thus, the strain rate can be estimated as 0.73 pct/s (i.e., $0.0011 \div 0.15$ seconds).

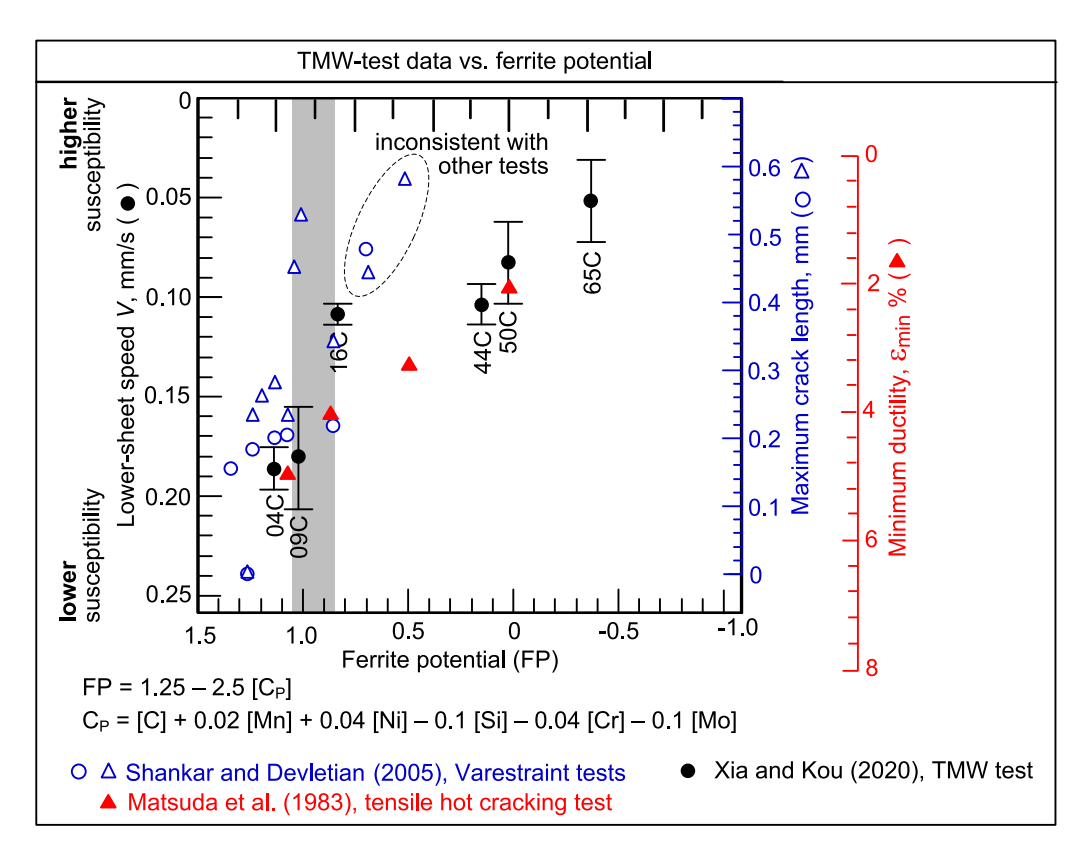


Fig. 8—Plotting results of TMW test, Varestraint tests, and tensile hot cracking test in Fig. 7 vs. ferrite potential.

Now consider the strain rate in the 09C-steel weld during the TMW test. The transition range for the lower-sheet V to change from no cracking to full cracking is from 0.155 to 0.208 mm/s, the midpoint of the range being about 0.18 mm/s. Since the width of the 09C-steel weld W is 4.4 mm, $^{[9]}$ the overall critical strain rate in the transverse direction across the width of the weld is 0.18 mm/s divided by 4.4 mm, that is, 0.041/s or 4.1 pct/s. This strain rate is much higher than the 0.73 pct/s strain rate caused by the $\delta \rightarrow \gamma$ transformation. In fact, it has been shown that the local critical strain rate near the crack is much higher than the overall critical strain rate across the width of the weld, about one order of magnitude higher. [41,42] Thus, it is likely that the strain rate caused by the $\delta \rightarrow \gamma$ transformation in carbon steels is less significant in welding than in casting.

Wolf^[43] introduced the following ferrite potential (FP) as a measure of the extent of the peritectic behavior experienced by a steel:

$$FP = 1.25 - 2.5[C_P],$$
 [1]

where the carbon equivalent C_P is defined as follows:

$$\begin{split} C_P = [C] + 0.02[Mn] + 0.04[Ni] - 0.1[Si] - 0.04[Cr] \\ - 0.1[Mo]. \end{split}$$

[2]

When FP is in the range of 0.85 to 1.05 (peritectic behavior range), the tendency for depressions, crack formation, and uneven shell growth is said to be high.

Table II shows the ferrite potentials calculated for the carbon steels used in the TMW test based on their compositions listed in Table I. The compositions of the carbon steels used by Shankar and Devletian[30] and their ferrite potentials are shown in Tables III and IV, respectively. Likewise, the compositions of the carbon steels used by Matsuda et al. [32] and their ferrite potentials are shown in Tables V and VI, respectively. Based on these tables, Figure 7 is replotted vs. the ferrite potential as shown in Figure 8. The shaded region represents the range of 0.85 to 1.05, in which the peritectic behavior is expected to be highest. As shown a peak crack susceptibility does exist in the range of ferrite potential between 0.85 and 1.05 as expected. However, below the range the crack susceptibility decreases with decreasing ferrite potential, instead of remaining roughly constant and well below the peak as expected in casting of carbon steels.[38]

Finally, it just came to the authors' attention that the index for the susceptibility to solidification cracking proposed by Kou^[10,11] has been applied by Guo and Wen^[26] recently to study hot tearing in steel ingots. Unlike the equilibrium solidification of binary Fe-C alloys considered in the present study, they considered multicomponent alloys and diffusion in calculating the index, which had been demonstrated previously by Liu and Kou for Al alloys.^[13] They concluded the index was useful for their study.

IV. CONCLUSIONS

By assuming equilibrium solidification of binary Fe-C alloys as an approximation for the solidification of carbon steels, the susceptibility of carbon steels to solidification cracking can be analyzed. The curve of the equilibrium freezing temperature range vs. the C content does not correlates well with the experimental data of the weldability tests of carbon steels. Based on equilibrium solidification and the maximum $|dT/d(f_S)^{1/2}|$ near $(f_S)^{1/2} = 1$ as the index for the susceptibility vs. the C content has been calculated. The curve agrees with the weldability tests of carbon steels.

ACKNOWLEDGMENTS

Chunzhi Xia was supported by the Jiangsu Overseas Visiting Scholar Program for University Prominent Young and Middle-aged Teachers and Presidents as a Visiting Professor at the University of Wisconsin-Madison from 2018 to 2019. Sindo Kou was supported by the National Science Foundation initially under Grant No. DMR 1500367 and subsequently under Grant No. DMR1904503.

REFERENCES

- S Kou: Welding Metallurgy, 3rd ed., Wiley, Hoboken, NJ, 2020, pp. 323–77.
- 2. WF Savage and CD Lundin: Weld. J., 1965, vol. 44, pp. 433s-42s.
- 3. T Soysal and S Kou: Weld. J., 2017, vol. 96, pp. 389s-401s.
- 4. T Soysal and S Kou: Acta Mater., 2018, vol. 143, pp. 181-97.
- T Soysal and S Kou: *J. Mater. Process. Technol.*, 2019, vol. 266, pp. 421–28.
- K Liu and S Kou: Sci. Technol. Weld. Join., 2020, vol. 25, pp. 251–57.
- 7. K. Liu, P. Yu, and S. Kou: Weld. J., 2020, vol. 99, pp. 255s-70s.
- C Xia and S Kou: Sci. Technol. Weld. Join., 2020, https://doi.org/ 10.1080/13621718.2020.1802897.
- C Xia and S Kou: Sci. Technol. Weld. Join., 2020, https://doi.org/ 10.1080/13621718.2020.1812211.
- 10. S Kou: Acta Mater., 2015, vol. 88, pp. 366-74.
- 11. S Kou: Weld. J., 2015, vol. 94, pp. 374s-88s.
- T Soysal and S Kou: Sci. Technol. Weld. Join., 2019, vol. 24, pp. 559–65.
- 13. J Liu and S Kou: Acta Mater., 2017, vol. 125, pp. 513-23.
- 14. J Liu, HP Duarte, and S Kou: *Acta Mater.*, 2017, vol. 122, pp. 47–
- 15. J Liu and S Kou: Acta Mater., 2016, vol. 110, pp. 84-94.
- 16. J Liu and S Kou: Acta Mater., 2015, vol. 100, pp. 359-68.
- AlcoTec Wire Corporation: Aluminum Filler Alloy Chart, AlcoTec Wire Corporation, Traverse, 2020. http://www.alcotec.com/us/en/

- support/upload/Aluminum_Filler_Alloy_Selection_Chart.pdf. Accessed 6 Aug 2020.
- Maxal International, Inc.: Maxal Guide for Aluminum Welding, Maxal International, Inc., Traverse, 2012. http://Maxal.com. Accessed 1 Aug 2012.
- N Coniglio and CE Cross: Metall. Mater. Trans. A, 2009, vol. 40A, pp. 2718–28.
- 20. J Campbell. *Castings*, 2nd ed., Butterworth Heinemann, Oxford, 2003, pp. 242–58.
- 21. J. Campbell: Private Communications, University of Birmingham, 2014.
- S Kou: Transport Phenomena and Materials Processing, Wiley, Hoboken, NJ, 1996, pp. 64–67.
- D.J. Fisher and W. Kurz: Unpublished Research, Department of Materials, EPFL-Swiss Institute of Technology, Lausanne, 1978.
- L Wang, N Wang, and N Provatas: *Acta Mater.*, 2017, vol. 126, pp. 302–12.
- 25. J Han, J Wang, M Zhang, and K Niu: *Materials*, 2019, vol. 5, p. 100203.
- 26. J Guo and G Wen: Metals, 2019, vol. 9, p. 836.
- P Rong, N Wang, L Wang, R Yang, and W Yao: *J. Alloy Compd.*, 2016, vol. 676, pp. 181–86.
- Computherm LLC: Pandat—Phase Diagram Calculation Software Package for Multicomponent Systems, Computherm LLC, Madison, 2020. https://www.computherm.com/. Accessed 1 May 2020.
- Computherm LLC: PanIron—Thermodynamic Database for Commercial Iron Alloys, Computherm LLC, Madison, 2020. http s://computherm.com/. Accessed 1 May 2020.
- 30. V Shankar and JH Devletian: Sci. Technol. Weld. Join., 2005, vol. 10, pp. 236-43.
- 31. T Senda, F Matsuda, G Takano, K Watanabe, T Kobayashi, and T Matsuzaka: *Trans. Jpn Weld. Soc.*, 1971, vol. 2, pp. 141–62.
- 32. F Matsuda, H Nakagawa, K Nakata, H Kohmoto, and Y Honda: *Trans. JWRI*, 1983, vol. 12, pp. 65–72.
- 33. S Ohshita, N Yurioka, N Mori, and T Kimura: *Weld. J.*, 1983, vol. 62, pp. 129s–36s.
- 34. T Amaya, T Yonezawa, K Ogawa, MJ Peltonen, and H Hanninen: *Weld. J.*, 2018, vol. 97, pp. 55s–64s.
- 35. RB Smith: *ASM Handbook. Welding, Brazing and Soldering*, ASM International, Materials Park, OH, 1993, vol. 6, pp. 641–61.
- G Poltarak, S Ferro, and C Cicutti: Steel Res. Int., 2017, vol. 88, p. 1600223.
- 37. Y Won, T Yeo, D Seol, and K Oh: *Metall. Mater. Trans. B*, 2000, vol. 31B, pp. 779–94.
- 38. G Azizi, B Thomas, and M Zaeem: *Metall. Mater. Trans. B*, 2020, vol. 51B, pp. 1875–1903.
- 39. M Wolf and W Kurz: *Metall. Trans. B*, 1981, vol. 12B, pp. 85–93.
- K Harste and K Schwerdtfeger: ISIJ Int., 2003, vol. 43, pp. 1011– 20.
- 41. T Soysal and S Kou: *Sci. Technol. Weld. Join.*, 2020, vol. 25, pp. 415–21.
- N Bakir, A Gumenyuk, and M Rethmeier: Sci. Technol. Weld. Join., 2018, vol. 23, pp. 234–40.
- 43. MM Wolf: in *Continuous Casting. Initial Solidification Strand Surface Quality of Peritectic Steels*, MM Wolf, ed., Iron and Steel Society/AIME, Warrendale, PA, 1997, vol. 9, pp. 61–65.

Publisher's Note Springer Nature remains neutral with regard to jurisdictional claims in published maps and institutional affiliations.